Ionic Liquids with Weakly Coordinating [M^{III}(OR^F)$_4$]$^-$ Anions

Alexander B. A. Rupp[†,‡] and Ingo Krossing*[,†,‡]

†Albert-Ludwigs-University Freiburg, Institute for Inorganic and Analytical Chemistry, Albertstrasse 21, 79104 Freiburg, Germany
‡Freiburg Materials Research Center, Stefan-Meier-Strasse 21, 79104 Freiburg, Germany

CONSPECTUS: Ionic liquids (ILs) are defined as salts with melting points below 100 °C. They attracted much attention in the last two decades due to their unique set of properties, including high conductivities, low viscosities, negligible vapor pressure, and high electrochemical resistance. ILs are seen as tunable systems, of which (also in mixtures) up to 10^{19} combinations may exist. These properties make ILs interesting candidates for a variety of fundamental to industrial applications. Our addition to this field was weakly coordinating, little interacting anions, the highly fluorinated aluminates [Al(OR^F)$_4$]$^-$ (R^F = C(CF$_3$)$_3$, C(CH$_3$), (CF$_3$)$_2$, and CH(CF$_3$)$_2$ and later also CH$_2$(CF$_3$)). We have used these anions in a broad spectrum of applications, including the stabilization of reactive cations, (polymerization) catalysis, and conducting salts for cyclic voltammetry or in electrochemical cells. Especially the [Al(Ohfip)$_4$]$^-$ (hfip = CH(CF$_3$)$_2$) anions in combination with asymmetric organic cations turned out to be very well suited for the synthesis of ILs with very low melting points, some even far below 0 °C. Also the analogous borates, [B(OR^F)$_4$]$^-$, were shown to yield ILs, and currently a plethora of such aluminate and borate ILs have been synthesized and thoroughly investigated. In many aspects, at least the [Al(Ohfip)$_4$]$^-$ ILs present almost ideally noninteracting prototype ILs with (nearly) isotropic but weak and flat Coulomb potential. Consequently, their overall interionic interactions are significantly reduced compared with other classes of ILs, resulting in an extraordinarily low degree, or (for short cation chain lengths below six) even complete absence of ion pairing. From thorough analysis of the principles governing the physical properties of this highly fluorinated IL class with minimized interactions, we were able to learn basic principles that could be extended, for example, to the prediction of the principal properties of a wide variety of typical ILs.

In this Account, we give a comprehensive review of their syntheses, thermal and toxicological behavior, physical as well as dynamic properties, and use in electrochemical applications. We delineate advantages and limitations of the [M^{III}(OR^F)$_4$]$^-$ ILs developed in our lab and give an outlook on those fields, in which there is still a lack of knowledge.
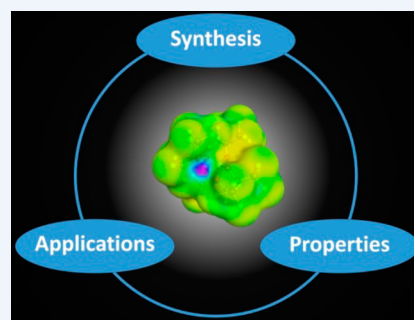
INTRODUCTION

The most prevalent definition of the term ionic liquid (IL), states that ILs are substances comprised merely of ions and having a melting point below 100 °C. With melting points below 25 °C, they are called room temperature ionic liquids (RTILs). The first ILs were described at the beginning of the 20th century by C. Schall and P. Walden.[1,2] IL research has been strongly expanding, and today many research activities in physics, life, and material science as well as chemistry take place.[3−12] Estimations including IL mixtures predict up to 10^{19} possible combinations of cations and anions forming ILs.[13,14] This large number offers a unique possibility for the fine-tuning of IL properties. Hence, predictive tools for IL properties get increasingly important. However, some types of ILs are plainly too different to subsume them.[15]

To achieve low melting points, the attractive interactions between cations and anions must be low to overcompensate the enthalpy of melting by the thermal energy. At the melting point, liquid and solid phase are in equilibrium, and thus $\Delta_{melt}G = 0$. This leads to eq 1, which describes the melting point (T_{melt}) as a function of the ratio of melting enthalpy ($\Delta_{melt}H$) and melting entropy ($\Delta_{melt}S$).

$$T_{melt} = \frac{\Delta_{melt}H}{\Delta_{melt}S} \tag{1}$$

The enthalpic part of eq 1 usually is dominated by Coulomb interactions, although dispersive forces and directed interactions (H-bonds etc.) are nonetheless important for the understanding of ILs.[16−19] From eq 2, where q_1 and q_2 are point charges in the distance r and ε_0 = vacuum permittivity, it follows that decreasing the charge and increasing the size of ions diminishes the overall electrostatic interaction, the Coulomb energy, E_C.

$$E_C = \frac{q_1 q_2}{4\pi\varepsilon_0 r} \tag{2}$$

$\Delta_{melt}H$ of ILs typically lies between 5 and 30 kJ·mol^{-1} but may reach 50 kJ·mol^{-1}.[20−22] Melting entropies are at least equally important or can indeed be the actual driving force for melting.[22,23]

But what is the actual difference between solid and liquid ILs that governs the temperature of the melting process? In a crystal lattice, ion movement including rotational degrees of freedom is restricted and according to Boltzmann's equation, $S = k_B \cdot \ln \Omega$, entropy is low in the solid state. This notion is crucial for asymmetric ions like [C$_n$MIm]$^+$ that potentially do have a large number of accessible conformations. During melting, however, conformational flexibility

increases and, for instance, alkyl chains can now undergo rotation around their C−C bonds, yielding access to all those low-lying conformations and thus providing entropy. Thus, in low melting ILs, the number of thermally accessible conformations of both anion and cation is high. These effects are included with the Gibb's energies in the phase-change Born−Fajans−Haber cycle in Scheme 1.

Scheme 1. Born−Fajans−Haber Cycle for the Calculation of the Gibbs Energy of Melting, $\Delta_{melt}G^a$
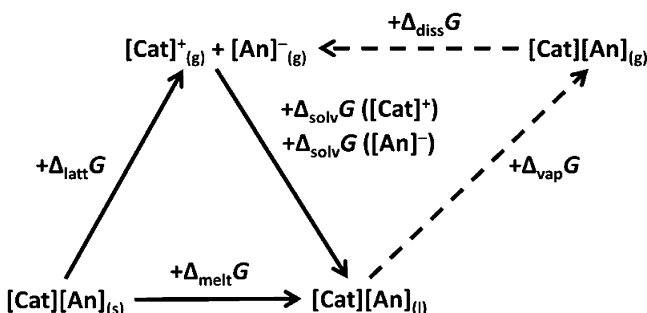
^{a}Cat = cation; An = anion; s = solid; l = liquid; g = gaseous; $\Delta_{latt}G$ = Gibbs lattice energy; $\Delta_{solv}G$ = Gibbs solvation energy; $\Delta_{diss}G$ = Gibbs dissociation energy; $\Delta_{vap}G$ = Gibbs vaporization energy.

With these phase-change thermodynamics in combination with quantum-mechanical calculations, we were able to understand and model the mentioned effects quantitatively, including the prediction of melting points.[20,24,25] Here, the model character of the weakly interacting $[M^{III}(OR^F)_4]^-$ ILs (M = B, Al; R^F = $C(CF_3)_3$, $C(CH_3)(CF_3)_2$, $CH(CF_3)_2$, $CH_2(CF_3)$) was crucial to understand the underlying physical relations. Next, we will first describe the synthesis and properties of these model ILs and then analyze and explain their diverse behavior.

■ SYNTHESES OF $[Cat][M^{III}(OR^F)_4]$ IONIC LIQUIDS

Similar to most IL classes, the general synthesis schemes toward $[Cat][M^{III}(OR^F)_4]$ ILs are not very difficult and follow Scheme 2. However, there are minor but important differences

Scheme 2. General Metathesis Reaction for the Formation of ILs with $[M^{III}(OR^F)_4]^-$ Anions
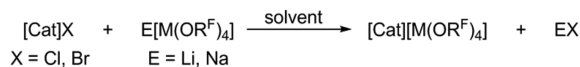
among the anions that are listed in Table 1. Interestingly, although all IL classes are easily soluble in dichloromethane, the metathesis of the borate anions only takes place in Et_2O or MeCN. In order to remove the alkali metal halide, the acetonitrile in the case of $[B(Otfe_4)]^-$ (tfe = CH_2CF_3) must be exchanged after the reaction with CH_2Cl_2 so that the byproduct can precipitate. Yields are in all cases well above 85%, and deviations from a quantitative yield often simply occur due to too short reaction times.

■ THERMAL BEHAVIOR

As with most IL classes, also $[M(OR^F)_4]^-$ ILs often are hard to crystallize and rather show glass transitions. Furthermore, they frequently possess a broad hysteresis leading to differing melting points, T_{melt}, by up to 30 °C and crystallization temperatures, T_c (cf. Table 2).[3] While this is only a kinetic effect, it can be beneficial for the investigation of ILs in their supercooled state: Thus, it was possible to measure the diffusion constants of $[C_2MIm][Al(Ohfip)_4]$ (hfip = $CH(CF_3)_2$) and $[C_4MIm][Al(Ohfip)_4]$ at room temperature, although their melting points are 31 and 41 °C, respectively.[3,30] However, replacing $[Al(Ohfip)_4]^-$ with $[Al(Opftb)_4]^-$ (pftb = $C(CF_3)_3$) leads to a sharp increase in the melting points. A similar but less pronounced increase is generated by exchanging $[Al(Ohfip)_4]^-$ with one of the two borate anions, $[B(Ohfip)_4]^-$ or $[B(Otfe)_4]^-$.

The thermal stability of $[Al(OR^F)_4]^-$ ILs[3,26] and $[B(OR^F)_4]^-$ ILs,[27] as investigated by DSC, showed that both classes of ILs exhibit decomposition temperatures, T_d, between 150 and 250 °C (cf. Table 2). Salts with the most stable $[Al(Opftb)_4]^-$ anions typically possess higher T_d and T_{melt} values than $[Al(Ohfip)_4]^-$ ILs. No thorough investigation on the decomposition products of these ILs was performed. However, from mass spectrometry studies it is known that $[Al(OR^F)_4]^-$ anions can decompose into $[F−Al(OR^F)_3]^-$, generating the respective volatile epoxides.[3,26] It is therefore reasonable to presume that under thermal decomposition, the same reactions take place.

■ TOXICOLOGICAL ASSESSMENT

The biodegradability of a small number of $[Al(Ohfip)_4]^-$ ILs was tested in *closed bottle tests* and *manometric respiratory tests*.[3,34] However, none of the four ILs was biodegradable under the aerobic conditions of the tests. On the other hand, no toxicity against bacteria could be observed either. Mechanistically, hydrolysis of $[Al(Ohfip)_4]^-$ releases the respective alcohol, HOhfip, which is relatively harmless toward animals and humans. Only its corrosiveness and the resulting irritation of skin and mucosa, originating from its relatively low aqueous pK_a of 9.5, need to be considered in terms of safety precautions. This result means that the release of these ILs into the environment should be prevented in order to avert long-time environmental effects.

■ DYNAMIC PROPERTIES AND INTERIONIC INTERACTIONS

Dynamic properties are of uttermost importance for many applications, with high diffusion constants, low viscosity, and high conductivity being mainly sought. In some areas, for example, lubrication research, also higher viscosities can be favorable. In the following, *viscosity* always means *dynamic viscosity*, while *conductivity* denotes *ionic conductivity*.

Viscosities

Room temperature viscosities, η, of $[Cat][M^{III}(OR^F)_4]$ ILs[3,26,28,29,33,38] approximately range from 30 to 1000 mPa·s and decrease to approximately 10 mPa·s at 80 °C.[29,30] First investigations of $[Al(Ohfip)_4]^-$ ILs concentrated on the quantitative,

Table 1. Reaction Conditions for the Synthesis of ILs of the Form $[Cat][M^{III}(OR^F)]$ via Metathesis According to Scheme 2

starting material	solvent	reaction time	purification	water/air sensitivity
Li[Al(Ohfip)₄][3,26]	CH_2Cl_2	0.5−24 h	centrifugation	high
Na[B(Ohfip)₄][27]	Et_2O	0.5−24 h	filtration	low
Li[Al(Opftb)₄][28]	CH_2Cl_2	0.5−24 h	centrifugation	none
Na[B(Otfe)₄][29]	MeCN; CH_2Cl_2	48 h	centrifugation	none

Table 2. Comparison of Physicochemical Data of Salts with Highly Fluorinated $[M(OR^F)_4]^-$ Anions[a]

IL	T_{melt}[31]	T_c	T_d	ε_r	η (40 °C)	σ (40 °C)	D^+	D^-	ionicity	VFT parameter (η)			VFT parameter (σ)		
										η_0	B	T_0	σ_0	B	T_0
Li[Al(Ohftb)$_4$]	42–45[31]														
Li[Al(Ohfip)$_4$]	120–125[31]														
Li[Al(Opftb)$_4$]	145–150[31]														
Li[B(Otfe)$_4$]		−35[32]	200[32]			0.014[b32]	48[b32]	43[b32]	0.0002[b32]						
Na[B(Ohfip)$_4$]·DME	56[27]	41	271[33]												
[C$_2$MIm][Al(Ohfip)$_4$]	31	<25	159	12.6	24.4	6.22	1.94	0.80	2.10[c]	0.0040	2402	38	1000	1258	68
[C$_2$MIm][Al(Otfe)$_4$]	35[29]	34			15.9					0.0889	795	160			
[C$_2$MMIm][Al(Ohfip)$_4$]	39	−24	172–176	18.0	22.4	6.86	4.77	1.89	0.87	0.0645	1031	146	96	206	255
[AllylMIm][Al(Ohfip)$_4$]	12	44		17.0						0.1066	905	144	93	241	220
[AllylMIm][B(Ohfip)$_4$]	68[27]	<25	172												
[C$_4$MIm][Al(Ohfip)$_4$]	40	42		14.5	21.8		2.20	1.30	1.03	0.430	1130	132	38	113	264
[C$_4$MIm][B(Ohfip)$_4$]	49[27]	−35	198							0.2190	619	204	0.083	1255	568
[C$_4$MMIm][Al(Ohfip)$_4$]	0	48		19.0	23.6	4.08	2.78	1.69	0.83	0.0985	852	157	558	830	145
[C$_4$MMIm][B(Ohfip)$_4$]	68[27]		221							1.572	206	266			
[C$_4$MMIm][B(Otfe)$_4$]	58[29]	−5								0.0442	926	203			
[C$_6$MIm][Al(Ohfip)$_4$]	5[34]			17.3	25.3	3.57	2.80	1.80	0.73	0.1743	709	170	32.0[d]	23.7[d]	
[C$_6$MIm][B(Ohfip)$_4$]	−25< T_{melt} < 0[27]				58.9	1.10				0.3590	593	197	14	165	250
[C$_6$MIm][B(Otfe)$_4$]	45[29]									0.0030	2020	129			
[C$_6$MIm][Al(Opftb)$_4$]	67[35]														
[C$_8$MIm][Al(Ohfip)$_4$]	<20				22.0	2.70	2.01	1.46	0.82	0.0134	1486	112	154	537	181
[C$_8$MIm][B(Otfe)$_4$]	28[29]									0.0066	1609	156			
[C$_{10}$MIm][Al(Ohfip)$_4$]	<20				25	2.10	1.60	1.29	0.79	0.0069	1716	104	294	796	152
[N$_{1111}$][Al(Ohfip)$_4$]	61[26]		147												
[N$_{1111}$][Al(Ohftb)$_4$]	96		>150												
[N$_{1111}$][Al(Opftb)$_4$]	320[26]		>400												
[N$_{1123}$][Al(Ohfip)$_4$]	43				30.4	2.00	1.21	0.97	0.87	0.1219	837	164	10.0[d]	20.5[d]	
[N$_{1444}$][Al(Ohfip)$_4$]	<20		>130												
[N$_{2222}$][Al(Ohfip)$_4$]	56[26]		>230												
[N$_{2222}$][Al(Ohftb)$_4$]	111		>400												
[N$_{2222}$][Al(Opftb)$_4$]	308[26]														
[N$_{4444}$][Al(Ohfip)$_4$]	42[26]		190		49.9					0.0552	946	163	259	713	167
[N$_{4444}$][Al(Ohftb)$_4$]	108		>150												
[N$_{4444}$][Al(Opftb)$_4$]	199[26]		>250												
[N$_{2225}$][Al(Ohfip)$_4$]	<20	−53[e]			34.4	2.77	2.10	1.50	0.69	0.1467	690	195	106	514	200
[N$_{2225}$][B(Otfe)$_4$]	89[29]														
[N$_{2666}$][Al(Ohfip)$_4$]	<20				35	0.92	0.73	0.76	0.80	0.0205	1269	142	116	431	199
[N$_{2666}$][B(Otfe)$_4$]	68[29]														
[N$_{1888}$][Al(Ohfip)$_4$]	<20	−53[e]			45.7	0.62	0.63	0.75	0.47	0.0432	1005	163	316	868	165
[N$_{1888}$][B(Otfe)$_4$]	4[29]				161					0.0102	1582	125	377	1021	155
[N$_{1888}$][Al(Opftb)$_4$]	<20				320.5					3.6×10^{-6}	3887	93			
[C$_3$MPip][Al(Ohfip)$_4$]	69	58													
[C$_4$MPyr][Al(Ohfip)$_4$]	50	39	155	16.6						0.0114	1823	135			

Table 2. continued

IL	T_{melt}	T_c	T_d	ε_r	η (40 °C)	σ (40 °C)	D^+	D^-	ionicity	VFT parameter (η)			VFT parameter (σ)		
---	---	---	---	---	---	---	---	---	---	η_0	B	T_0	σ_0	B	T_0
[C$_4$MMorph][Al(Ohfip)$_4$]	31	6	164	16.5	41.3	1.99				4.2×10^{-5}	4198	10			
[C$_4$MMorph][B(Ohfip)$_4$]	113[27]	102	256	16.5	25.1					0.1952	623	185			
[C$_4$Py][Al(Ohfip)$_4$]	36	<25													

$^a T_{melt}$ = melting temperature (°C); T_c = crystallization temperature (°C); T_d = decomposition temperature (°C); ε_r = dielectric constant (Cole–Cole model); η = viscosity (mPa·s); σ = ionic conductivity (mS·cm^{-1}); D = diffusion constants (10^{-11} m^2·s^{-1}); η_0 = viscosity at infinite temperature (mPa·s), B = constant (K); T_0 = Vogel temperature (K); σ_0 = conductivity at infinite temperature. η_0, σ_0, B, T_0 are defined according to eqs 3c and 3f. hftb = C(CF$_3$)$_2$(CH$_3$). ^{b}Measured at 130 °C. ^{c}Measured in a highly supercooled state. ^{d}Due to mathematical instabilities, an Arrhenius fit of the form $\sigma = \sigma_0 \exp(-B/(RT))$, where R = universal gas constant, T = absolute temperature, σ_0 is given in S·cm^{-1}, and B is given in kJ·mol^{-1}, was used. ^{e}Glass transition.

temperature-dependent viscosity description[34] by Arrhenius (eqs 3a, viscosity, and 3d, conductivity), Litovitz (eqs 3b, viscosity, and 3e, conductivity), and Vogel–Fulcher–Tammann (VFT; eqs 3c, viscosity, and 3f, conductivity)) approaches.

$$\eta = \eta_0 \exp\left(\frac{E_A^{visc}}{RT}\right) \tag{3a}$$

$$\eta = \eta_0 \exp\left(\frac{B}{RT^3}\right) \tag{3b}$$

$$\eta = \eta_0 \exp\left(\frac{B}{T - T_0}\right) \tag{3c}$$

$$\sigma = \sigma_0 \exp\left(-\frac{E_A^{cond}}{RT}\right) \tag{3d}$$

$$\sigma = \sigma_0 \exp\left(-\frac{B}{RT^3}\right) \tag{3e}$$

$$\sigma = \sigma_0 \exp\left(-\frac{B}{T - T_0}\right) \tag{3f}$$

where E_A = activation energy, R = universal gas constant, T = absolute temperature, η_0 = viscosity at infinite temperature, σ_0 = conductivity at infinite temperature, B = a substance-specific constant, and T_0 = Vogel temperature.

In principal, all three models yield good results. The best description, however, was achieved with the VFT ansatz. Therefore, in all following studies VFT models were used (VFT parameters given in Table 2). Two larger studies of [Al(Ohfip)$_4$]$^-$ ILs allowed for a thorough understanding of the molecular mechanisms governing viscosities.[3,30] Viscosities strictly decrease with temperature and show a tendency to increase with increasing molecular volume of the cation. Thus, by going from [N$_{2225}$][Al(Ohfip)$_4$] ($V_m^+ = 0.322$ nm^3) to [N$_{1888}$][Al(Ohfip)$_4$] ($V_m^+ = 0.604$ nm^3), the viscosity at 25 °C increases from 69.5 to 94 mPa·s.[30] Compared with [NTf$_2$]$^-$ ILs (Tf = SO$_2$CF$_3$), a much lower cation dependence is observed: The difference between [N$_{2225}$][NTf$_2$] (175 mPa·s) and [N$_{1888}$][NTf$_2$] (600 mPa·s) is 2.5-fold larger![30]

For the higher melting of [B(Ohfip)$_4$]$^-$ salts, not many viscosity data are known.[27] However, data of the [C$_4$MIm]$^+$, [C$_4$MMIm]$^+$ and [C$_6$MIm]$^+$ salts indicate that viscosities are well above those of respective [Al(Ohfip)$_4$]$^-$ ILs. Compared to other classes of ILs, viscosities of [Al(Ohfip)$_4$]$^-$ ILs are below or in the range of [NTf$_2$]$^-$ ILs, while [B(Ohfip)$_4$]$^-$ ILs rather resemble the more viscous [BF$_4$]$^-$ ILs.[36] Ionic liquids with [B(Otfe)$_4$]$^-$ anions have been characterized only recently.[29] [B(Otfe)$_4$]$^-$ salts also show much higher viscosities than [Al(Ohfip)$_4$]$^-$ ILs, reaching values of roughly 1000 mPa·s at 20 °C. Although such high viscosities restrict the use of pure [B(Otfe)$_4$]$^-$ ILs as electrolytes, it may well be that their general chemical stability—also toward water and air—is beneficial for an application as e.g. lubricants. In addition, mixtures of Li[B(Otfe)$_4$] and molecular solvents were shown to be promising for an application in lithium sulfur batteries.[33] The last subclass, [Al(Opftb)$_4$]$^-$ ILs, have rather high melting points. In fact, only one RTIL comprising [Al(Opftb)$_4$]$^-$, [N$_{1888}$][Al(Opftb)$_4$] has been discovered so far. Its room temperature viscosity is 824 mPa·s, with a decrease down to 50 mPa·s at 80 °C, while the respective viscosities for its [Al(Ohfip)$_4$]$^-$ analogue are 94 mPa·s and 10 mPa·s. It appears

that $[Al(Opftb)_4]^-$ salts exhibit higher viscosities compared to the other $[M^{III}(OR^F)_4]^-$ IL classes.

Conductivities

Conductivity data very much resemble those of viscosities. Conductivities, σ, of $[M^{III}(OR^F)_4]^-$ ILs are best fitted with a VFT approach, although an Arrhenius ansatz is also well applicable here.[3] Again, $[Al(Ohfip)_4]^-$ ILs prove to be the best subclass with conductivities of up to 4 mS·cm^{-1} at 25 °C.[3,30] As with the viscosities, the effect of exchanging cations is relatively negligible compared with $[NTf_2]^-$ ILs.[30] Imidazolium-based ILs show superior properties compared with ammonium ILs. Altogether, the same trends as in the case of viscosities seem to prevail,[27] and a similar order can be deduced with some caution: $\sigma([Al(Ohfip)_4]^-) > \sigma([B(Ohfip)_4]^-) \approx \sigma([B(Otfe)_4]^-) > \sigma([Al(Opftb)_4]^-)$.

Walden Plots

From conductivities and viscosities, Walden plots can be extracted. Walden plots are double logarithmic plots of (molar) conductivity and fluidity (inverse viscosity). A diluted KCl solution defines the "ideal" line, suggesting a complete lack of ion pairing.[37] Ionic liquids being above the ideal line are termed *super ILs*, whereas ILs below the ideal line are divided into *good ILs* and *poor ILs*, depending on the distance from the ideal line. However, the use of the KCl line as an ideal reference system has been questioned not only due to its arbitrary character but also because it is not a highly diluted solution, exhibits ion pairing, and in fact would possess a slope of 0.87 instead of 1 if precise experimental data was used.[38] Still, it is widely used in the literature. The distance from the KCl line is supposed to correlate with the ionicity, which is a measure for the availability of ions in an electrolyte.[39] As visualized in Figure 1, both $[Al(Ohfip)_4]^-$
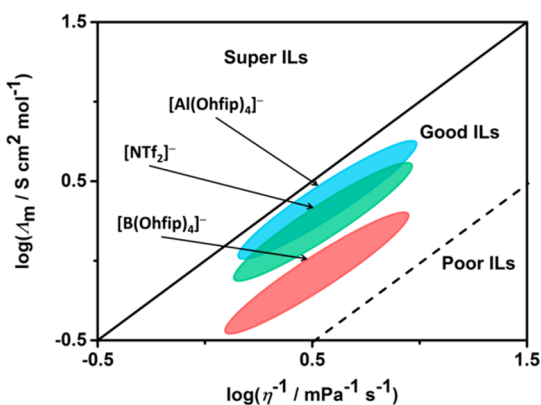
Figure 1. Schematic Walden plot with typical regions of nonfunctionalized $[Al(Ohfip)_4]^-$ and $[B(Ohfip)_4]^-$ ILs in comparison to $[NTf_2]^-$ ILs. Λ_m = molar conductivity.

and $[B(Ohfip)_4]^-$ ILs are good ILs.[3,27] In fact, some $[Al(Ohfip)_4]^-$ ILs are even better than $[C_2MIm][NTf_2]$ and $[C_4MIm][NTf_2]$, two of the best commercially available ILs. In other words, $[Al(Ohfip)_4]^-$ ILs use their potential almost fully, while $[NTf_2]^-$ ILs lose some of their conductivity potential due to ion-pairing processes (see below).

Self-Diffusion Constants and Ion-Pairing

Self-diffusion constants can be conveniently measured via pulsed field gradient NMR experiments. In the case of ILs, one has to take care of the pulse sequence, since some techniques impose uncertainties due to T_2 relaxation.[40] A comparative study of

diffusion constants of 12 $[Al(Ohfip)_4]^-$ ILs and their $[NTf_2]^-$ analogues yielded the ion-specific diffusion constants given in Table 2.[30] From first principles, one would probably assume that $[NTf_2]^-$ ILs should show larger diffusion constants due to their smaller molecular volume and lower molar mass. However, a more complex picture arises from the diffusion data. Obviously, not only are cations faster in almost all $[Al(Ohfip)_4]^-$ ILs than in the respective $[NTf_2]^-$ ILs, but also the $[Al(Ohfip)_4]^-$ anions themselves have larger diffusion constants than $[NTf_2]^-$ anions, despite their 2.5 times larger volume. Applying a modified Stokes−Einstein equation, eq 4, to the diffusion data allowed for a semiquantitative comparison of $[NTf_2]^-$ and $[Al(Ohfip)_4]^-$ ILs.

Generalized Stokes−Einstein Equation

$$\frac{D^+}{D^-} = A(V_m^+)^{-b} \tag{4}$$

where D^+ = cation diffusion constant, D^- = anion diffusion constant, A = a constant, V_m^+ = cation molecular volume, and b = a constant. In the case of ideal Stokes−Einstein behavior, $b = 1/3$.

The exponent b was associated with the predominant interaction in the ILs.[30] For $[Al(Ohfip)_4]^-$ and $[NTf_2]^-$ ILs, $b = 0.91$ and $b = 0.63$, respectively, were found. Our interpretation suggests that in $[NTf_2]^-$ ILs, a significant amount of surface-mediated interactions such as dispersion interactions are present, while $[Al(Ohfip)_4]^-$ ILs barely show any further interactions apart from weak, isotropic electrostatic interactions (see discussion later). This notion can be further supported by combining conductivity and diffusion data and using the definition of ionicity suggested by the group of Watanabe.[41−43] This definition relies on the assumption that ion-pairing processes are too fast to be detected on the NMR time scale. Hence, only an average signal per ion species is detected comprising both paired and unpaired ions. Contrarily, during conductivity measurements only unpaired ions contribute to conductivity. Therefore, if diffusion constants are converted into conductivities using the Nernst−Einstein equation, an (apparent) upper conductivity limit is calculated. The quotient of measured and calculated conductivity then defines the ionicity, eq 5; that is, it is a measure for the share of unpaired ions.

Equation for the Calculation of Ionicities, I

$$I = \frac{\sigma_{exp}}{\sigma_{diff}} = \frac{\sigma_{exp}MkT}{e^2\rho N_A(D^+ + D^-)} \tag{5}$$

where σ_{exp} = experimentally measured conductivities, σ_{diff} = conductivities calculated from diffusion constants, D, M = molar mass, k = Boltzmann's constant, T = absolute temperature, e = elementary charge, ρ = density, and N_A = Avogadro's constant.

Calculating ionicities of $[Al(Ohfip)_4]^-$ ILs yields values that are in almost all cases considerably higher than those of $[NTf_2]^-$ ILs.[30] Consequently, this observation leads to the conclusion that ion-pairing clearly is less favored in $[Al(Ohfip)_4]^-$ ILs than in $[NTf_2]^-$ ILs.

Dielectric Properties

We measured the dielectric constants of several $[Al(Ohfip)_4]^-$ ILs with dielectric relaxation spectroscopy (Cole−Cole (CC) model, included with Table 2) and surprisingly found ε_r to be

relatively high compared with that of $[NTf_2]^-$ ILs.[3,44] Since gaseous $[Al(Ohfip)_4]^-$ actually exhibits a higher symmetry than $[NTf_2]^-$ (S_4 vs C_2), the net dipole moment of S_4-symmetric $[Al(Ohfip)_4]^-$ would be expected to be zero, and thus the higher dielectric constants of $[Al(Ohfip)_4]^-$ ILs were unexpected. We concluded that this phenomenon could mainly be attributed to a reduction in symmetry of the anion in the liquid state. A similar distortion was verified in crystal structures. Thus, when the frozen conformations of the solid $[Al(Ohfip)_4]^-$ anion in the IL crystals were used for single point dipole moment calculations with DFT methods, the calculated dipole moment differed strongly from zero and reached values between 0.5 and 3.7 D.[3] The existence of long-lived ion pairs, which would contribute to ε_r due to their high dipole moment, could be excluded on the time scale of the experiment (down to 2 ps). Thus, it appears that the high conformational flexibility of the $[Al(Ohfip)_4]^-$ ILs led to a large percentage of long-lived conformations with a higher net dipole moment of the anion, which overall led to the higher dipole density necessary to induce these unexpectedly high static dielectric constants.

Another issue, relevant for the analysis and interpretation of other dynamic measurements, is the applicability of hydrodynamic models in the case of ILs. The use of such models for the description of reorientational dynamics in ILs was addressed with dielectric relaxation spectroscopy of $[Al(Ohfip)_4]^-$ ILs:[45] We found that the width parameter α in the CC model was low ($\alpha = 0.13-0.30$), indicating the presence of heterogeneities formed by hydrophilic and hydrophobic domains in the ILs.[45,46] Additionally, the calculation of effective volumes, V_{eff}, and coupling factors, f, as defined by $f = V_{eff}/V$, led to low coupling factors in the range of 10^{-2} to 10^{-3}, also in the cases of $[N(CN)_2]^-$, $[BF_4]^-$, $[PF_6]^-$, and $[NTf_2]^-$ ILs. This is consistent with almost frictionless rotational motion or *slip conditions* in the hydrodynamic description. Due to the very low friction, we concluded that, although the applicability of hydrodynamic models cannot be ruled out, such models should only be used with caution, since phenomena like jump diffusion may play a role in the dynamic behavior of ILs.

■ DISCUSSION OF THE BEHAVIOR OF $[M^{III}(OR^F)_4]^-$ IONIC LIQUIDS

Almost all mentioned physicochemical observations could be traced back to few basic principles: large ion size reduces electrostatic contributions, while hardly polarizable surface atoms diminish dispersive and Lewis interactions. From these considerations follows that a good choice for the ions of an ionic liquid can be made by relying on the following rules:

- The ions' absolute charge must be small and should be delocalized over several atoms.
- Conformational flexibility should be high to increase melting entropy.
- The ions should have no strongly Lewis-basic or Lewis-acidic sites.
- The surface should mainly comprise hardly polarizable surface atoms (i.e., fluorine).

The $[M(OR^F)_4]^-$ anions fulfill these criteria to a great extent. Exemplarily, molecular volumes, melting points of the respective rather symmetric $[NEt_4]^+$ salts, and the symmetry descriptors σ and τ[23] governing their melting behavior are collected in Table 3.

All anions have very similar values of V_m and σ, but melting points that range from 56 to 308 °C. $[NEt_4]^+[Al(Opftb)_4]^-$ only differs from the other salts in τ, which depends[23] on the number

Table 3. Comparison of Molecular Volumes (V_m), Symmetry Numbers (σ), Torsional Freedom Factors (τ), and Melting Points (T_{melt}) of Highly Fluorinated Aluminate Anions and Their $[NEt_4]^+$ Salts

	$[Al(Opftb)_4]^-$	$[Al(Ohftb)_4]^-$	$[Al(Ohfip)_4]^-$
V_m, nm^3[23]	0.747	0.667	0.581
σ[23]	4	4	4
τ[23]	3	7	7
T_{melt}, °C ($[NEt_4]^+$ salts)[26]	308	111	56

of torsion angles that lead to a new conformation. This τ-value is significantly smaller for this most symmetric and actually largest anion with the therefore smallest Coulomb potential. *Thus, only based on enthalpic Coulomb considerations, one would expect this salt to have the lowest melting point.* However, the C_s symmetric hfip and tfe residues contribute more to the overall entropy of the IL than pftb residues with a local symmetry of C_{3v} (Figure 2).
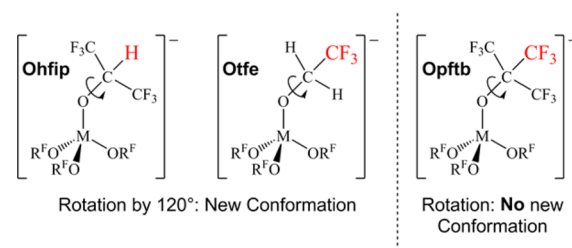
Figure 2. Differences in the rotational degrees of freedom of Ohfip, Otfe, and Opftb residues.

Consequently, $[Al(Opftb)_4]^-$ ILs exhibit much higher melting points and viscosities as well as lower conductivities and diffusion constants. The differences between $[Al(Ohfip)_4]^-$ and $[B(Ohfip)_4]^-$ could also be attributed to entropy, because the shorter B−O bonds lead to steric hindrance and limit the accessibility of the rotational degrees of freedom. The slightly higher melting points of $[B(Otfe)_4]^-$ salts probably originate from the lower percentage of fluorinated surface area, which creates potentially Lewis acidic sites (H atoms) and less effectively screens potentially Lewis basic sites (O atoms), as underlined by electrostatic potentials of the anions (Figure 3).
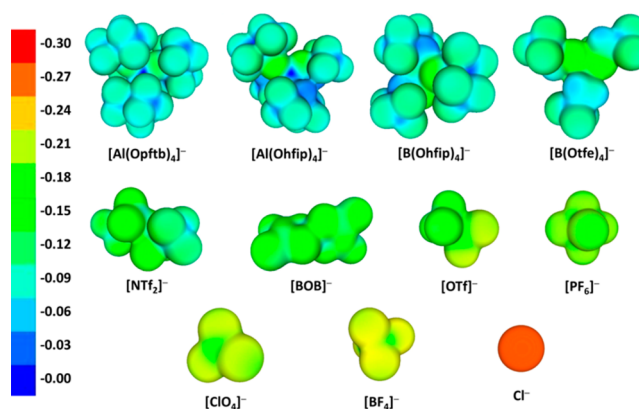
Figure 3. Electrostatic potentials (in atomic units) of $[M(OR^F)_4]^-$ and other anions for comparison. Calculations were performed on a RI-BP-86/TZVP level of theory. BOB = bis-oxalatoborate(III).

Accordingly, melting points show the order $[Al(Ohfip)_4]^- < [B(Ohfip)_4]^- \approx [B(Otfe)_4]^- < [Al(Opftb)_4]^-$. With this reasoning,

also other effects are easily explained: Longer alkyl chains, for instance, lead to higher entropy and larger holes in the ion packing but also increase dispersive interactions and thus eventually lead to a deterioration of desired properties. Therefore, nonlinear behavior is observed, with ILs comprising medium-sized cations possessing lower melting points than ILs with both small and large cations.

The difference between $[\text{Cat}][\text{M}^{\text{III}}(\text{OR}^{\text{F}})_4]$ and other ILs can now also be elucidated. In contrast to $[\text{Al}(\text{Ohfip})_4]^-$, $[\text{NTf}_2]^-$ still has Lewis-basic surface atoms (N, O) and a considerably smaller diameter, leading to stronger and more individual interionic interaction and causing not only the mentioned cation dependence of viscosity but also higher activation barriers for ion movement processes (Figure 4).[30]
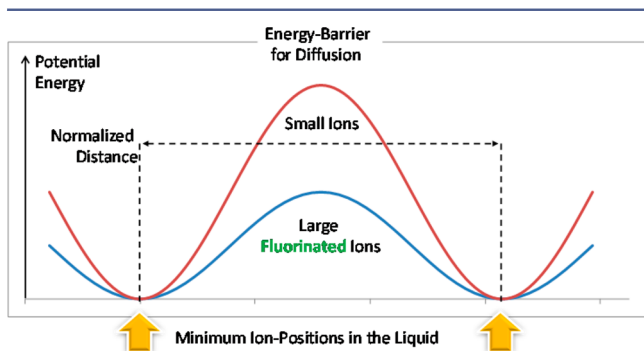
Figure 4. Energy barriers of ions diffusing in an IL.

Another consequence is that viscosities of $[\text{Al}(\text{Ohfip})_4]^-$ ILs are typically lower than those of $[\text{NTf}_2]^-$ ILs. Moreover, also ionicities underline this explanation, with $[\text{Al}(\text{Ohfip})_4]^-$ ILs possessing in general explicitly higher ionicities than their $[\text{NTf}_2]^-$ counterparts.

■ MODIFICATIONS OF STANDARD [Cat][M$^{\text{III}}$(OR$^{\text{F}}$)$_4$] IONIC LIQUIDS

Functionalizations

For $[\text{NTf}_2]^-$ and other common ILs, various cation functionalizations are known.[47−50] However, only few modifications were introduced into $[\text{Cat}][\text{M}^{\text{III}}(\text{OR}^{\text{F}})_4]$ ILs.[3,27,51] These will be briefly discussed here.

A common and quite simple modification is the introduction of a double bond into the side chain of imidazolium cations, for instance, in the $[\text{AllylMIm}]^+$ cation. Although this does not result in a fully delocalized system, it nevertheless changes the electronic structure and modes of interaction in the IL. Experiments and calculations on both $[\text{AllylMIm}][\text{Al}(\text{Ohfip})_4]$[3,30] and $[\text{AllylMIm}][\text{B}(\text{Ohfip})_4]$[27] have been conducted and showed that $[\text{AllylMIm}][\text{Al}(\text{Ohfip})_4]$ has a remarkably high dipole moment compared with other $[\text{C}_n\text{MIm}][\text{Al}(\text{Ohfip})_4]$ salts of similar volume.[3] It also possesses lower melting and crystallization temperatures than $[\text{C}_n\text{MIm}][\text{Al}(\text{Ohfip})_4]$ ILs, albeit the melting entropy should actually be reduced due to the rigidity of the double bond (!). Furthermore, it shows the lowest room temperature viscosity, highest conductivity, and largest diffusion constants of all $[\text{M}(\text{OR}^{\text{F}})_4]^-$ ILs. Obviously, the introduction of the allyl residue can strongly alter properties.

Another modification, investigated with T. Welton and P. Lickiss, is the introduction of siloxane residues.[51] Two $[\text{Al}(\text{Ohfip})_4]^-$ ILs with siloxane cations shown in Figure 5 have been prepared and were compared with analogue $[\text{NTf}_2]^-$ ILs.
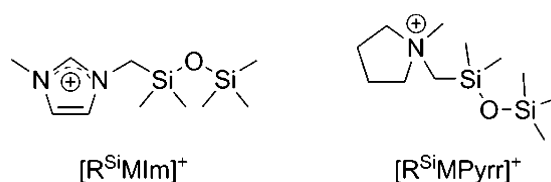
Figure 5. Siloxane-modified cations.

Viscosities of these $[\text{Al}(\text{Ohfip})_4]^-$ ILs are comparable to or somewhat smaller than those of nonfunctionalized ILs, while conductivities are smaller. $[\text{R}^{\text{Si}}\text{MIm}][\text{Al}(\text{Ohfip})_4]$, for instance, exhibits a viscosity of 34 mPa·s and a conductivity of 1.23 mS·cm^{-1} at 298 K, whereas $[\text{C}_6\text{MIm}][\text{Al}(\text{Ohfip})_4]$ shows values of 43.5 mPa·s and 2.36 mS·cm^{-1}, respectively. Notably, both siloxane-comprising $[\text{Al}(\text{Ohfip})_4]^-$ ILs are less viscous than their $[\text{NTf}_2]^-$ counterparts but equally conducting. Vogel–Fulcher–Tammann fits of viscosities and conductivities yielded no abnormality. This result is in accordance with the high conformational flexibility of Si–O units.

Mixtures

We investigated the influence of dimethylcarbonate (DMC) on $[\text{M}(\text{Ohfip})_4]^-$ ILs, with a focus on conductivity, viscosity, and diffusion constants.[52] DMC was chosen due to its good electrochemical stability, its low viscosity, and its low permittivity of $\varepsilon_{\text{r}} = 3.12$,[53] which typically would rule out DMC as solvent for salts. Quite in contrast, addition of DMC to the $[\text{M}(\text{Ohfip})_4]^-$ ILs with a weak and flat Coulomb potential resulted in a pronounced increase of conductivity and diffusion constants, while viscosity decreased with DMC content. However, these trends were not linearly connected to one another: A 10-fold increase in diffusion constants by going from $[\text{N}_{1123}][\text{Al}(\text{Ohfip})_4]\cdot0.55\text{DMC}$ to $[\text{N}_{1123}][\text{Al}(\text{Ohfip})_4]\cdot2.76\text{DMC}$ only produced a roughly 3.5-fold increase in conductivity. Furthermore, the order in conductivity was partially reversed in the case of diffusion constants. These peculiarities were explained with ionicity and viscosity data: High DMC contents correlated with low ionicities. This is due to the small permittivity of DMC and the thus lower stabilization of free electric charge according to Coulomb's law. On the other hand, viscosities always decreased considerably upon addition of DMC. Overall the following holds: As DMC is added, viscosity decreases, which would ultimately lead to an extensive increase in ion mobility. Simultaneously, ions tend to form more ion pairs or higher-order aggregates of the general form $[\text{Cation}]_x[\text{Anion}]_{x\pm1}^{\mp}$, which not only reduces the number of available net charge carriers but also leads to lower diffusion constants of these larger aggregates. A comprehensive overview of ion pairing in mixtures of imidazolium ionic liquids with molecular solvents was given recently by Stassen, Ludwig, Wulf, and Dupont.[54]

■ APPLICATION OF [Al(Ohfip)$_4$]$^-$ IONIC LIQUIDS AS ELECTROLYTES

Since $[\text{Al}(\text{Ohfip})_4]^-$ ILs exhibited very good dynamic properties, we investigated their potential application as electrolytes in supercapacitors in comparison to conventional $[\text{NTf}_2]^-$ ILs.[55] Supercapacitors have two electrodes, a separator membrane, and the electrolyte and store energy by the separation of opposite charges on the electrodes.[56] We first used microporous activated carbon electrodes with a surface area of approximately 1700 m^2·g^{-1} and a binder-free glass microfiber filter as separator. With this setup, we were able to reproduce literature values for $[\text{C}_2\text{MIm}][\text{NTf}_2]$.[57] However, compared with the gravimetric

capacitance of 134 F·g^{-1} for $[C_2MIm][NTf_2]$ and 77 F·g^{-1} for $[C_4MIm][NTf_2]$, only very low values of 11 F·g^{-1} at the most were reached for the tested $[Al(Ohfip)_4]^-$ ILs. Since basic dynamic properties did not suggest such a large difference, we exchanged the electrodes with meso- and macroporous electrodes to further investigate this behavior. Although, as expected, gravimetric capacitance deteriorated for all electrolytes due to the smaller specific surface area, a clear equalization between $[NTf_2]^-$ and $[Al(Ohfip)_4]^-$ ILs was observed with gravimetric capacitances of roughly 10 F·g^{-1}. These data allowed for insight into the underlying effects: ILs[3,58,59] screen electric charge effectively within short distance. Hence, to screen virtually the complete charge at the electrode surface, only a first layer of counterions is needed. Consequently, accessibility of pores for the ions of the ILs is crucial to exploit the full electrode capacitance. Here, the large size of $[Al(Ohfip)_4]^-$ anions proves an obstacle in the case of micropores, leading to a reduction in the effective accessible surface area for the IL ions in the range of 97.5%. However, when this *sieving effect* is eliminated, for example, with optimized porous electrode materials, $[Al(Ohfip)_4]^-$ ILs become competitive in terms of gravimetric capacitance compared with $[NTf_2]^-$ ILs. Ideally, $[Al(Ohfip)_4]^-$ ILs would need electrodes with pore sizes of 1.1−1.2 nm and a rather narrow pore size distribution in order to maximize gravimetric surface area, accessibility of pores, and stabilization of charges by IL ions.

CONCLUSION AND OUTLOOK

This Account summarizes the synthesis, properties, and understanding of highly fluorinated $[M^{III}(OR^F)_4]^-$ ionic liquids. Fundamental knowledge about interionic interaction within ionic liquids was generated. However, still some questions are to be addressed in the future, including the role of mixtures between different ILs or the use of fluorinated cations with $[M^{III}(OR^F)_4]^-$ salts. Possible applications of these ILs in the future include lubricants, additives, or electrolytes in electrochemical cells and conductive salts for electrochemical measurements in moderately polar solvents.

AUTHOR INFORMATION

Corresponding Author

*E-mail: ingo.krossing@ac.uni-freiburg.de.

Notes

The authors declare no competing financial interest.

Biographies

Alex Rupp studied chemistry at the Albert-Ludwigs-Universität Freiburg and finished his Ph.D. degree in Freiburg under the supervision of Prof. Ingo Krossing in early 2015. He is a fellow of the Studienstiftung Deutschen Volkes, and his scientific interests reach from synthesis of ionic liquids to the understanding of their principal physical and electrochemical properties.

Ingo Krossing studied chemistry at the LMU in Munich and finished his Ph.D. thesis in the group of Prof. H. Nöth in 1997. As a Feodor Lynen Fellow, he worked with the inorganic fluorine chemist Prof. J. Passmore at UNB, Canada. In 1999, he started his independent scientific career on the development and use of weakly coordinating anions (WCAs) as a Liebig-Fellow and later a DFG-Heisenberg-Fellow at the Universität Karlsruhe (TH) (associated with Prof. H. Schnöckel). An assistant professor position at the Ecole Polytechnic Federale de Lausanne (EPFL) was the next station in 2004. In 2006, he took over the Chair of Inorganic and Molecular Chemistry at the Albert-Ludwigs-Universität Freiburg. His research interests cover ionic systems from reactive cations, to strong Brønsted and Lewis acids, over preparation, understanding, and prediction in the field of ionic liquids, as well as electrolytes for electrochemical energy storage. He is currently a recipient of the ERC Advanced Grant UniChem developing absolute acidity and reducity scales.

ACKNOWLEDGMENTS

ABBREVIATIONS

$[C_nMIm]^+$ = 1-methyl-3-n-alkylimidazolium cations where n denotes the number of carbon atoms in the n-alkyl chain
$[N_{abcd}]^+$ = tetra-n-alkylammonium cations, where a, b, c, and d denote the number of C atoms in each n-alkyl chain
hfip = $CH(CF_3)_2$
hftb = $C(CF_3)_2(CH_3)$
pftb = $C(CF_3)_3$
tfe = CH_2CF_3
Tf = SO_2CF_3

REFERENCES

(1) Schall, C. Über organische und geschmolzene Salze. *Z. Elektrochem. Angew. Phys. Chem.* **1908**, *14*, 397−405.

(2) Walden, P. Ueber die Molekulargrösse und elektrische Leitfähigkeit einiger geschmolzenen Salze. *Bull. Acad. Imp. Sci. St.-Petersbourg* **1914**, *6*, 405−422.

(3) Bulut, S.; Klose, P.; Huang, M.-M.; Weingärtner, H.; Dyson, P. J.; Laurenczy, G.; Friedrich, C.; Menz, J.; Kümmerer, K.; Krossing, I. Synthesis of Room-Temperature Ionic Liquids with the Weakly Coordinating $[Al(OR^F)_4]^-$ Anion (R^F = $C(H)$ $(CF_3)_2$) and the Determination of Their Principal Physical Properties. *Chem. - Eur. J.* **2010**, *16*, 13139−13154.

(4) Anderson, J. L.; Dixon, J. K.; Brennecke, J. F. Solubility of CO_2, CH_4, C_2H_6, C_2H_4, O_2, and N_2 in 1-Hexyl-3-methylpyridinium Bis(trifluoromethylsulfonyl)imide: Comparison to Other Ionic Liquids. *Acc. Chem. Res.* **2007**, *40*, 1208−1216.

(5) Tan, S.; Ji, Y. J.; Zhang, Z. R.; Yang, Y. Recent Progress in Research on High-Voltage Electrolytes for Lithium-Ion Batteries. *ChemPhysChem* **2014**, *15*, 1956−1969.

(6) Kar, M.; Simons, T. J.; Forsyth, M.; MacFarlane, D. R. Ionic liquid electrolytes as a platform for rechargeable metal-air batteries: a perspective. *Phys. Chem. Chem. Phys.* **2014**, *16*, 18658−18674.

(7) Plechkova, N. V.; Seddon, K. R. Applications of ionic liquids in the chemical industry. *Chem. Soc. Rev.* **2008**, *37*, 123−150.

(8) MacFarlane, D. R.; Tachikawa, N.; Forsyth, M.; Pringle, J. M.; Howlett, P. C.; Elliott, G. D.; Davis, J. H.; Watanabe, M.; Simon, P.; Angell, C. A. Energy applications of ionic liquids. *Energy Environ. Sci.* **2014**, *7*, 232−250.

(9) Arbizzani, C.; Lazzari, M.; Soavi, F.; Mastragostino, M.; Conte, M. ILHYPOS Ionic Liquid-Based Supercapacitors. *ECS Trans.* **2010**, *25*, 25−30.

(10) Minami, I. Ionic Liquids in Tribology. *Molecules* **2009**, *14*, 2286−2305.

(11) Cao, Y.; Wu, J.; Zhang, J.; Li, H.; Zhang, Y.; He, J. Room temperature ionic liquids (RTILs): A new and versatile platform for cellulose processing and derivatization. *Chem. Eng. J. (Amsterdam, Neth.)* **2009**, *147*, 13−21.

(12) Moniruzzaman, M.; Goto, M. Ionic Liquids: Future Solvents and Reagents for Pharmaceuticals. *J. Chem. Eng. Jpn.* **2011**, *44*, 370−381.

(13) Holbrey, J. D.; Seddon, K. R. Ionic Liquids. *Clean Technol. Environ. Policy* **1999**, *1*, 223−236.

(14) Izgorodina, E. I. Towards large-scale, fully ab initio calculations of ionic liquids. *Phys. Chem. Chem. Phys.* **2011**, *13*, 4189−4207.

(15) McCrary, P. D.; Rogers, R. D. 1-Ethyl-3-methylimidazolium hexafluorophosphate: from ionic liquid prototype to antitype. *Chem. Commun. (Cambridge, U. K.)* **2013**, *49*, 6011−6014.

(16) Zahn, S.; Uhlig, F.; Thar, J.; Spickermann, C.; Kirchner, B. Intermolecular Forces in an Ionic Liquid ([Mmim][Cl]) versus Those in a Typical Salt (NaCl). *Angew. Chem., Int. Ed.* **2008**, *47*, 3639−3641.

(17) Tsuzuki, S.; Tokuda, H.; Hayamizu, K.; Watanabe, M. Magnitude and Directionality of Interaction in Ion Pairs of Ionic Liquids: Relationship with Ionic Conductivity. *J. Phys. Chem. B* **2005**, *109*, 16474−16481.

(18) Kempter, V.; Kirchner, B. The role of hydrogen atoms in interactions involving imidazolium-based ionic liquids. *J. Mol. Struct.* **2010**, *972*, 22−34.

(19) Fumino, K.; Reimann, S.; Ludwig, R. Probing molecular interaction in ionic liquids by low frequency spectroscopy: Coulomb energy, hydrogen bonding and dispersion forces. *Phys. Chem. Chem. Phys.* **2014**, *16*, 21903−21929.

(20) Preiss, U.; Verevkin, S. P.; Koslowski, T.; Krossing, I. Going Full Circle: Phase-Transition Thermodynamics of Ionic Liquids. *Chem. - Eur. J.* **2011**, *17*, 6508−6517.

(21) Domańska, U. Physico-Chemical Properties and Phase Behaviour of Pyrrolidinium-Based Ionic Liquids. *Int. J. Mol. Sci.* **2010**, *11*, 1825−1841.

(22) Carvalho, P. J.; Ventura, S. P. M.; Batista, M. L. S.; Schröder, B.; Goncalves, F.; Esperanca, J.; Mutelet, F.; Coutinho, J. A. P. Understanding the impact of the central atom on the ionic liquid behavior: Phosphonium vs ammonium cations. *J. Chem. Phys.* **2014**, *140*, 064505.

(23) Preiss, U.; Bulut, S.; Krossing, I. In Silico Prediction of the Melting Points of Ionic Liquids from Thermodynamic Considerations: A Case Study on 67 Salts with a Melting Point Range of 337 °C. *J. Phys. Chem. B* **2010**, *114*, 11133−11140.

(24) Krossing, I.; Slattery, J. M.; Daguenet, C.; Dyson, P. J.; Oleinikova, A.; Weingärtner, H. Why Are Ionic Liquids Liquid? A Simple Explanation Based on Lattice and Solvation Energies. *J. Am. Chem. Soc.* **2006**, *128*, 13427−13434.

(25) Beichel, W.; Preiss, U. P.; Verevkin, S. P.; Koslowski, T.; Krossing, I. Empirical description and prediction of ionic liquids' properties with augmented volume-based thermodynamics. *J. Mol. Liq.* **2014**, *192*, 3−8.

(26) Raabe, I.; Wagner, K.; Guttsche, K.; Wang, M.; Grätzel, M.; Santiso-Quiñones, G.; Krossing, I. Tetraalkylammonium Salts of Weakly Coordinating Aluminates: Ionic Liquids, Materials for Electrochemical Applications and Useful Compounds for Anion Investigation. *Chem. - Eur. J.* **2009**, *15*, 1966−1976.

(27) Bulut, S.; Klose, P.; Krossing, I. Na[B(hfip)₄] (hfip = OC(H)(CF₃)₂): a weakly coordinating anion salt and its first application to prepare ionic liquids. *Dalton Trans.* **2011**, *40*, 8114−8124.

(28) Rupp, A. B. A.; Priester, D.; Scherer, H.; Klose, P.; Koslowski, T.; Krossing, I. Manuscript in preparation.

(29) Rupp, A. B. A.; Klose, P.; Scherer, H.; Krossing, I. New Water-Stable Ionic Liquids Based on Tetrakis-(2,2,2-trifluoroethoxy)borate. *ChemPhysChem* **2014**, *15*, 3729−3731.

(30) Rupp, A.; Roznyatovskaya, N.; Scherer, H.; Beichel, W.; Klose, P.; Sturm, C.; Hoffmann, A.; Tübke, J.; Koslowski, T.; Krossing, I. Size matters! On the Way to Ionic Liquid Systems without Ion Pairing. *Chem. - Eur. J.* **2014**, *20*, 9794−9804.

(31) Krossing, I. The Facile Preparation of Weakly Coordinating Anions: Structure and Characterisation of Silverpolyfluoroalkoxyaluminates AgAl(OR^F)₄, Calculation of the Alkoxide Ion Affinity. *Chem.- Eur. J.* **2001**, *7*, 490−502.

(32) Tokuda, H.; Tabata, S.-i.; Susan, M. A. B. H.; Hayamizu, K.; Watanabe, M. Design of Polymer Electrolytes Based on a Lithium Salt of a Weakly Coordinating Anion to Realize High Ionic Conductivity with Fast Charge-Transfer Reaction. *J. Phys. Chem. B* **2004**, *108*, 11995−12002.

(33) Rohde, M.; Eiden, P.; Leppert, V.; Schmidt, M.; Garsuch, A.; Semrau, G.; Krossing, I. Li[B(OCH₂CF₃)₄]: Synthesis, Characterization and Electrochemical Application as a Conducting Salt for LiSB Batteries. *ChemPhysChem* **2015**, *16*, 666−675.

(34) Bulut, S.: Novel Ionic Liquids with Weakly Coordinating Anions: Synthesis, Characterization, Principal Physical Properties and Their Predictions PhD Thesis, Albert-Ludwigs-Universität, 2010.

(35) Rupp, A. B. A.: Investigations on Dynamic Properties of Ionic Liquids towards their Applications as Electroytes. Ph.D. Dissertation, Albert-Ludwigs-University, 2014.

(36) de Riva, J.; Ferro, V. R.; del Olmo, L.; Ruiz, E.; Lopez, R.; Palomar, J. Statistical Refinement and Fitting of Experimental Viscosity-to-Temperature Data in Ionic Liquids. *Ind. Eng. Chem. Res.* **2014**, *53*, 10475−10484.

(37) Yoshizawa, M.; Xu, W.; Angell, C. A. Ionic Liquids by Proton Transfer: Vapor Pressure, Conductivity, and the Relevance of pKa from Aqueous Solutions. *J. Am. Chem. Soc.* **2003**, *125*, 15411−15419.

(38) Schreiner, C.; Zugmann, S.; Hartl, R.; Gores, H. J. Fractional Walden Rule for Ionic Liquids: Examples from Recent Measurements and a Critique of the So-Called Ideal KCl Line for the Walden Plot. *J. Chem. Eng. Data* **2010**, *55*, 1784−1788.

(39) MacFarlane, D. R.; Forsyth, M.; Izgorodina, E. I.; Abbott, A. P.; Annat, G.; Fraser, K. On the concept of ionicity in ionic liquids. *Phys. Chem. Chem. Phys.* **2009**, *11*, 4962−4967.

(40) Annat, G.; MacFarlane, D. R.; Forsyth, M. Transport Properties in Ionic Liquids and Ionic Liquid Mixtures: The Challenges of NMR Pulsed Field Gradient Diffusion Measurements. *J. Phys. Chem. B* **2007**, *111*, 9018−9024.

(41) Ueno, K.; Tokuda, H.; Watanabe, M. Ionicity in ionic liquids: correlation with ionic structure and physicochemical properties. *Phys. Chem. Chem. Phys.* **2010**, *12*, 1649−1658.

(42) Tokuda, H.; Hayamizu, K.; Ishii, K.; Susan, M. A. B. H.; Watanabe, M. Physicochemical Properties and Structures of Room Temperature Ionic Liquids. 1. Variation of Anionic Species. *J. Phys. Chem. B* **2004**, *108*, 16593−16600.

(43) Noda, A.; Hayamizu, K.; Watanabe, M. Pulsed-Gradient Spin-Echo ¹H and ¹⁹F NMR Ionic Diffusion Coefficient, Viscosity, and Ionic Conductivity of Non-Chloroaluminate Room-Temperature Ionic Liquids. *J. Phys. Chem. B* **2001**, *105*, 4603−4610.

(44) Daguenet, C.; Dyson, P. J.; Krossing, I.; Oleinikova, A.; Slattery, J.; Wakai, C.; Weingärtner, H. Dielectric Response of Imidazolium-Based Room-Temperature Ionic Liquids. *J. Phys. Chem. B* **2006**, *110*, 12682−12688.

(45) Huang, M.-M.; Bulut, S.; Krossing, I.; Weingärtner, H. Communication: Are hydrodynamic models suited for describing the reorientational dynamics of ions in ionic liquids? A case study of methylimidazolium tetra(hexafluoroisopropoxy)aluminates. *J. Chem. Phys.* **2010**, *133*, 101101.

(46) Triolo, A.; Russina, O.; Bleif, H.-J.; Di Cola, E. Nanoscale Segregation in Room Temperature Ionic Liquids. *J. Phys. Chem. B* **2007**, *111*, 4641−4644.

(47) Li, X.; Zhao, D.; Fei, Z.; Wang, L. Applications of functionalized ionic liquids. *Sci. China, Ser. B: Chem.* **2006**, *49*, 385−401.

(48) Wong, W.-L.; Wong, K.-Y. Recent development in functionalized ionic liquids as reaction media and promoters. *Can. J. Chem.* **2012**, *90*, 1−16.

(49) Luska, K. L.; Moores, A. Functionalized Ionic Liquids for the Synthesis of Metal Nanoparticles and their Application in Catalysis. *ChemCatChem* **2012**, *4*, 1534−1546.

(50) Wang, C.; Luo, X.; Zhu, X.; Cui, G.; Jiang, D.-e.; Deng, D.; Li, H.; Dai, S. The strategies for improving carbon dioxide chemisorption by functionalized ionic liquids. *RSC Adv.* **2013**, *3*, 15518−15527.

(51) Bulut, S.; Ab Rani, M. A.; Welton, T.; Lickiss, P. D.; Krossing, I. Preparation of [Al(hfip)₄]⁻-Based Ionic Liquids with Siloxane-Functionalized Cations and Their Physical Properties in Comparison with Their [Tf₂N]⁻ Analogues. *ChemPhysChem* **2012**, *13*, 1802−1805.

(52) Rupp, A. B. A.; Welle, S.; Klose, P.; Scherer, H.; Krossing, I. Effect of Dimethyl Carbonate on the Dynamic Properties and Ionicities of Ionic Liquids with [M^III(hfip)₄]⁻ (M = B, Al) anions. *ChemPhysChem* **2015**, *16*, 1940−1947.

(53) McEwen, A. B.; McDevitt, S. F.; Koch, V. R. Nonaqueous Electrolytes for Electrochemical Capacitors: Imidazolium Cations and

Inorganic Fluorides with Organic Carbonates. *J. Electrochem. Soc.* **1997**, *144*, L84−L86.

(54) Stassen, H. K.; Ludwig, R.; Wulf, A.; Dupont, J. Imidazolium Salt Ion Pairs in Solution. *Chem. - Eur. J.* **2015**, *21*, 8324−8335.

(55) Roznyatovskaya, N.; Rupp, A. B. A.; Tübke, J.; Krossing, I. Sieving Effects in Electric Double-Layer Capacitors Based on Neat $[\mathrm{Al(hfip)_4}]^-$ and $[\mathrm{NTf_2}]^-$ Ionic Liquids. *ChemElectroChem* **2015**, *2*, 829−836.

(56) Conway, B. E. *Electrochemical Supercapacitors: Scientific Fundamentals and Technological Applications*; Springer: Berlin, 1999.

(57) Lewandowski, A.; Olejniczak, A.; Galinski, M.; Stepniak, I. Performance of carbon-carbon supercapacitors based on organic, aqueous and ionic liquid electrolytes. *J. Power Sources* **2010**, *195*, 5814−5819.

(58) Weingärtner, H. The Static Dielectric Constant of Ionic Liquids. *Z. Phys. Chem.* **2006**, *220*, 1395−1405.

(59) Weingärtner, H. Understanding Ionic Liquids at the Molecular Level: Facts, Problems, and Controversies. *Angew. Chem., Int. Ed.* **2008**, *47*, 654−670.